# Microscopic mechanisms of surface phase transitions on InAs(001)

Frank Grosse,[1,2] William Barvosa-Carter,[1,2] Jennifer J. Zinck,[1] and Mark F. Gyure[1]
[1]*HRL Laboratories LLC, 3011 Malibu Canyon Road, Malibu, California 90265*
[2]*Department of Mathematics, University of California, Los Angeles, California 90095-1555*
(Received 21 August 2001; revised manuscript received 25 April 2002; published 15 August 2002)

Microscopic mechanisms of the $(2\times4)$ to $(4\times2)$ surface phase transition on InAs(001) are identified using a combination of theoretical and experimental methods. Two distinct transition stages are found, both rate limited by $As_2$ desorption. The unusually high prefactors observed experimentally are traced back to the microscopic $As_2$ desorption processes. Calculated interactions between As dimers explain the observed disorder of the mixed $\alpha2(2\times4)$ and $\beta2(2\times4)$ reconstructions and are not responsible for observed first order behavior of the transition.

DOI: 10.1103/PhysRevB.66.075321 PACS number(s): 68.35.Rh, 68.35.Bs, 68.35.Ja, 68.35.Md

## I. INTRODUCTION

Understanding phase transitions on surfaces is of fundamental scientific interest as well as important for many technological applications. For semiconductor surfaces especially, a full microscopic understanding of reconstruction transitions is desirable, but difficult to attain due to their complex nature. Only in special cases can experimental data alone unambiguously identify elementary surface processes. As we will demonstrate, the application of modern theoretical and simulation methods, in combination with available experimental techniques, can enable a significantly deeper understanding of the microscopic processes underlying these transitions.

A common and intriguing feature of the (001) surfaces of all III-V semiconductor compounds is the wide variety of surface reconstructions (phases) differing in symmetry and stoichiometry that are observable, e.g., in molecular beam epitaxy (MBE), at different temperature and group V fluxes. For the (001) surface of group III arsenides (AlAs, GaAs, InAs), for instance, a $(2\times4)$ symmetry is observed under a wide range of flux conditions. In the metal rich regime, a $(4\times2)$ phase appears. Recent *ab initio* calculations using density functional theory (DFT) have clarified the stability[1–6] and qualitative similarity of the arsenide surface reconstructions.[2,4] The *transitions* between these reconstructions, however, have several interesting features, none of which are understood at a microscopic level. For example, GaAs(001) changes reconstruction from $(2\times4)$ to $(4\times2)$ continuously as a function of temperature, while the same transition is first order for InAs(001).[7] These changes in surface phase are intimately linked to the adsorption and desorption of arsenic, a subject of study since the inception of MBE.[8,9] The desorbing molecule was identified to be $As_2$ (Refs. 10 and 11) whereas the experimentally determined prefactors for desorption from $(2\times4)$ surfaces range from $10^{13}$ $s^{-1}$ for GaAs(001) to the unusually high value of $10^{19}$ $s^{-1}$ for InAs(001).[11] These facts suggest that more complicated processes than simple $As_2$ desorption might control the $(2\times4)$ to $(4\times2)$ phase transition. In spite of this interesting behavior, however, even the simple question of whether As or In kinetics controls these processes has not been conclusively answered.

The prefactor $\nu$ and activation energy $E_A$ of the $As_2$ desorption process for InAs(001) surfaces have been measured previously using mass spectrometry and reflection high-energy electron diffraction (RHEED).[11,12] Assuming a single process, the data were fitted to

$$\Gamma = \nu \exp(-E_A/k_BT), \tag{1}$$

where $\Gamma$ is the desorption rate, $T$ is the surface temperature, and $k_B$ is the Boltzmann constant. The prefactor deduced by Sasaoka, Kato, and Usui[11] was $\nu=10^{19}$ $s^{-1}$, anomalously high in comparison to prefactors for other desorption processes, typically in the range of $10^{12}$ to $10^{14}$ $s^{-1}$. Their fit with $E_A=2.86$ eV only agreed at high temperatures with the measured data. Liang and Tu[12] determined two activation energies for a high- and low-temperature range. Indeed, large discrepancies in reported activation energies are found in the literature ranging from 1.6 to 3.0 eV.[12–14]

To investigate the microscopic processes involved in the InAs(001) $(2\times4)$ to $(4\times2)$-reconstruction transition we have employed an interactive combination of DFT calculations and kinetic Monte Carlo (KMC) simulations together with scanning tunneling microscopy (STM) and RHEED measurements. We find that the transition can be divided into two distinct stages both rate limited by $As_2$ desorption kinetics: (I) a $\beta2(2\times4)$ to $\alpha2(2\times4)$ transition consisting only of simple single As-dimer desorption and (II) an $\alpha2(2\times4)$ to $(4\times2)$ transition accompanied by In sublattice rearrangement. In addition, we find that the interactions between As dimers in the $(2\times4)$ reconstruction contradict explanations of the first order phase transition for InAs(001).[7,15] It also follows that no ordered phase within the $\alpha2(2\times4)$-$\beta2(2\times4)$ reconstruction regime exists at finite temperature.

We employ the following methodology in this study. Time-dependent RHEED intensity measurements are used to monitor changes associated with the structure of the InAs(001) surface observed under a zero As flux condition. Two distinct stages of the $(2\times4)$ to $(4\times2)$ transition are revealed. STM images show that initially the surface has the $\beta2(2\times4)$ reconstruction, then transforms into $\alpha2(2\times4)$, and finally into a metal rich $(4\times2)$ reconstruction. We furthermore study static, annealed InAs(001) surfaces under

 

constant As flux by STM. The microscopic processes involved are investigated theoretically using DFT calculations and kinetic Monte Carlo (KMC) simulations based on DFT-determined energies. The prefactor for As desorption is determined by direct comparison of the KMC simulation results to STM data for annealed surfaces at fixed As flux. Finally we independently check our simulation results by comparing to annealed surfaces under different As flux and to the initial desorption experiment under zero flux conditions.

## II. EXPERIMENTS

Two different kinds of experiments are carried out to investigate the As kinetics on the InAs(001) surface. First, we study the dynamics of an initially As-rich surface under zero As flux. Second, surfaces are annealed under fixed finite As flux and the static surfaces are then investigated by STM.

We prepare As-rich surfaces of InAs(001) on undoped buffer layers ($>0.5$ $\mu$m thick) grown at 470°C on undoped InAs(001) substrates using conventional techniques in a VG 80H (Ref. 16) machine. The magnitude of the incident flux from the valved EPI $As_2$ source is measured by the uptake method.[17] The surface symmetry and changes in morphology are monitored using the diffraction and specular features of *in situ* RHEED at 13 keV and a nominal 1° angle of incidence. Photoemission (PE) from the InAs surface, generated by 5–7 eV photons from a $D_2$ lamp, is simultaneously monitored.[18]

To investigate the kinetics of the $(2\times4)$ to $(4\times2)$ transition, the InAs surface is stabilized in the As-rich $(2\times4)$ regime. The surface is then allowed to convert to $(4\times2)$ by closing the $As_2$ valve and shutter. The experiment is carried out at different temperatures. Upon cessation of the direct $As_2$ flux, we observe that the surface symmetry in RHEED stays $(2\times4)$ initially while the specular spot loses intensity (stage I in Fig. 1). A minimum in the specular spot intensity is reached after which the intensity of the (0,1/4) order streak observed in the [110] azimuth begins to increase sharply, indicating that the surface is converting to $(4\times2)$ (stage II). Under the diffraction conditions used the (0,1/4) order streak appears as a concentric light spot and will be called the $4\times$ feature in the following discussion. A similar behavior is noted in the PE signal as well, and the results are reported elsewhere.[19] The qualitative behavior is unchanged within the temperature range investigated here (380°–470°C).

In order to understand the variations in surface structure that are responsible for the observed changes in the RHEED and PE, several surfaces were studied using STM. Samples were quenched from a steady-state annealing condition by simultaneously shutting off the substrate heater power, closing the shutter and valve on the $As_2$ source, and rotating the sample towards the cryopanel. The samples were transferred in UHV through a gated transfer tube to a connected analysis chamber containing an Omicron LS full-wafer STM where they were subsequently imaged at room temperature. The first sample was prepared with RHEED and PE signals that matched those observed at the initial state of the surface (i.e., just prior to shuttering the As source). As shown in Fig. 2(a)

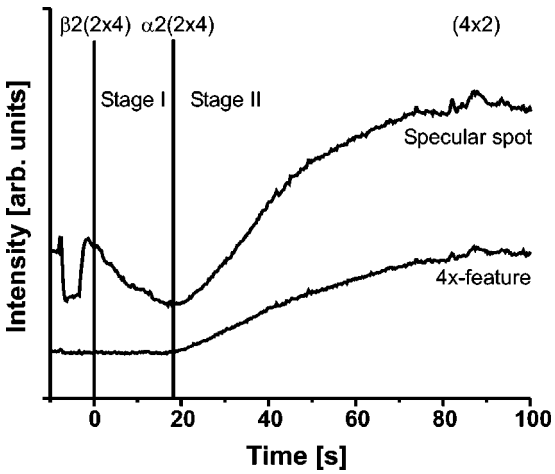


FIG. 1. Evolution of RHEED intensity during the $(2\times4)$-$(4\times2)$ transition at $T=430$°C. To reduce background $As_2$ effects, the starting surface is stabilized in the $(2\times4)$ regime with the lowest possible $As_2$ flux and then "dosed" by quickly opening the valve to $F_{As}=2.4$ ML/s for 2 sec (resulting in the initial dip and recovery in intensity), and then shuttering and closing the valve.

we clearly observe the double dimer rows associated with the $\beta2(2\times4)$ reconstruction. The second sample, shown in Fig. 2(b), was produced using RHEED and PE signals that matched those just prior to the observation of $(4\times2)$ as shown in Fig. 1. An atomic resolution STM image of a surface containing $\beta2(2\times4)$ as well as $\alpha2(2\times4)$ unit cells is presented in Fig. 3. On the basis of the high resolution images we are able to clarify structures of surfaces as presented in Fig. 2.

From these STM results, we clearly observe a loss of top-layer As dimers at lower $As_2$ fluxes, indicating that prior to formation of the $(4\times2)$ phase, the surface transforms to a primarily $\alpha2(2\times4)$ structure. The microscopic structure for both the $\alpha2(2\times4)$ and $\beta2(2\times4)$ reconstructions is schematically shown in Fig. 4. We have confirmed that these are indeed the most stable and likely structures for this surface, both by DFT (Ref. 4) and by atomic-resolution STM.[20] These observations strongly suggest that the desorption experiments can be rather simply interpreted: At the initial stage, the surface is clearly $\beta2(2\times4)$ whereas a primarily

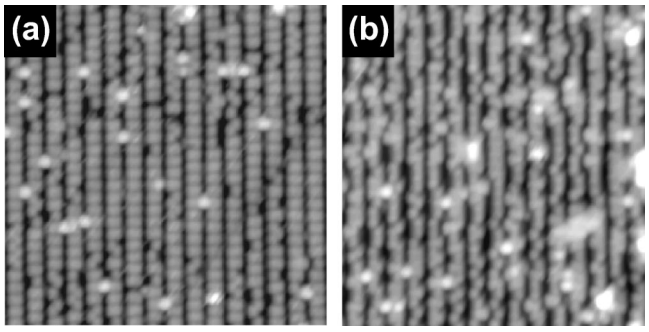


FIG. 2. Filled-states constant current STM image (2.5V bias, 0.05 nA) of an InAs(001) surface annealed at 420°C for 20 min with (a) $F_{As}=0.8$ ML/s and (b) $F_{As}=0.02$ ML/s.

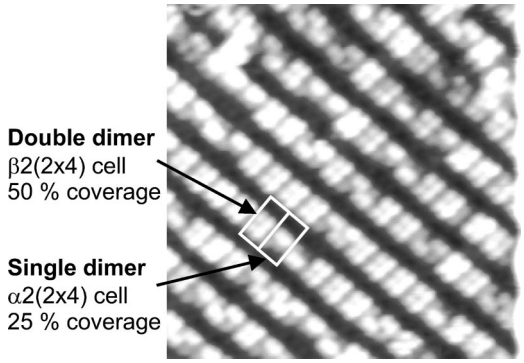


FIG. 3. Atomic resolution filled-state constant current STM image (1.3 V bias, 0.05 nA) of an InAs(001) surface annealed at 380 °C for 60 min with $F_{As}=0.08$ ML/s. Special unit cells are marked and the corresponding As coverage in the top layer is given.

$\alpha 2(2\times4)$ surface is observed at the minimum in the RHEED specular intensity shown in Fig. 1.

Aside from the reconstructed units on the surface, we find that there are numerous larger, nonperiodic defect structures such as trench-filling defects and bright ''on-row'' features that appear to sit either symmetrically or asymmetrically atop the dimer rows, as well as more extended, islandlike structures. Similar structures have also been observed previously on InAs surfaces[21] quenched $\approx$100 times faster than our estimated quench rate of 2–3°C/sec. We have done numerous experiments to trace the source of these features. For instance, the quantity of these features does not correlate with extended exposure to post-anneal conditions in the growth chamber, transfer tube, or STM chamber. In fact, there appears to be a slight tendency for the overall population to decrease with increased time at the anneal temperature. The strongest correlation appears to be with substrate temperature and the magnitude of the As flux after the anneal: we observe fewer of the larger structures at either higher As flux or decreased anneal temperature.

This correlation suggests that these features may be connected to an equilibrium adatom population.[22] The surface adatom concentration theoretically should have a similar dependence on anneal conditions, and this has been observed experimentally for GaAs.[23] However, unlike the observations on GaAs, these extended structures, while sometimes spanning several dimer rows, fall short of appearing as *reconstructed* islands when quenching from moderate anneal temperatures (380-430°C). Only quenching from higher temperatures (>440°C) appears to produce morphologies similar to those observed for GaAs. We feel that these features, while ubiquitous, do not have a disproportionate effect on our desorption measurements. If indeed these structures represent stable adatom complexes, then they will disrupt at most a few percent of the surface.

In stage II of the phase transition, the surface changes from $\alpha 2(2\times4)$ to a $(4\times2)$ reconstructed surface. Using the time dependence of the $4\times$ diffraction feature, measured from $T=430$ to 490°C, we determined the activation energy for the $\alpha 2(2\times4)$ to $(4\times2)$ transition to be $2.8\pm0.2$ eV. The corresponding prefactor obtained from the experimental data is $\nu=10^{19}$ $s^{-1}$.

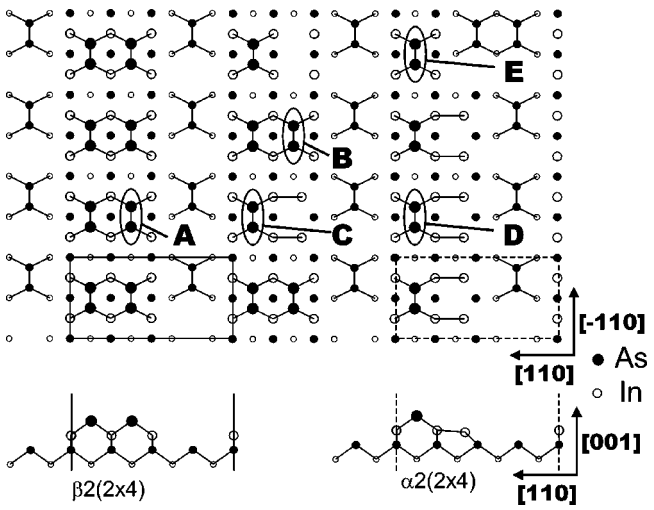


FIG. 4. Adsorption sites of As dimers on $\alpha 2(2\times4)$-$\beta 2(2\times4)$ reconstructed surfaces. The determined adsorption energies are $E(A)=2.48$ eV, $E(B)=2.48$ eV, $E(C)=3.19$ eV, $E(D)=3.19$ eV, $E(E)=2.8$ eV. The $\beta 2(2\times4)$ (solid line) and $\alpha 2(2\times4)$ (dashed) unit cells are marked and given with their respective side view.

## III. DENSITY FUNCTIONAL THEORY CALCULATIONS

To investigate $As_2$ desorption from InAs(001) theoretically, we first calculate energies for As dimers bonded to InAs(001)-$(2\times4)$ surfaces employing DFT calculations. These calculations are carried out within the generalized gradient approximation (GGA) using *ab initio* norm-conserving pseudopotentials.[24–26] Energies and structural data are converged with respect to cell size. Wave functions are expanded in a plane wave basis with a converged cutoff energy of 12 Ry and integrated using an equivalent set of 64 **k** points per $(1\times1)$ cell. A slab geometry with periodic boundary conditions is used consisting of the converged thickness of eight atomic layers for each vacuum and slab with the back surface passivated by pseudohydrogen. All layers are allowed to relax except the bottom.

The As dimer bond energy to the surface is defined as the total energy difference between the situation where the molecule is in the vacuum and where it is adsorbed on the surface. The local configurations seen by an As dimer can vary. Figure 4 depicts several $As_2$ adsorption sites on $(2\times4)$ reconstructed surfaces with calculated bond energies as described in the caption. Comparing the bond energies of sites A and B we find that the effective interaction between As dimers in the $[\bar{1}10]$ direction is negligible. The interaction in the [110] direction is therefore given by the difference of the bond energies of sites A and C or, equivalently, B and D, resulting in a repulsive interaction of 0.71 eV between dimers on next neighbor sites. Tests on $(2\times8)$ cells show that there is no effective interaction between the top As dimers in adjacent $(2\times4)$ cells in the [110] direction. These anisotropic interactions are understandable, given the microscopic structure. Neighboring As dimers in the [110] direc-

tion share a common In pair that constrains any subsequent relaxation leading to an effective repulsive interaction. In contrast, As dimer neighbors in the $[\bar{1}10]$ direction share only a second nearest neighbor in a bulklike bonding situation which has only a negligible effect.

Interestingly, neither next-neighbor dimer interaction agrees even qualitatively with the same interactions for GaAs(001) determined by Itoh *et al.*[27] using KMC simulations fit to STM data; both interactions were found to be positive. Furthermore, the electrostatic interaction between the filled dangling bonds of the As dimers in the $[\bar{1}10]$ direction appears to be fully screened. Therefore it is questionable whether arguments explaining total energy differences between reconstructions solely by electrostatic interactions due to charge transfer[1] are applicable here.

The lack of any interaction between dimers along the $[\bar{1}10]$ direction reveals another important fact: The $\alpha 2(2\times4)$ and $\beta 2(2\times4)$ reconstructions are not, in a thermodynamic sense, different phases of the surface. Describing the surface by an Ising-type model, where every spin represents a $(2\times4)$ cell, the interaction parameter is zero in both directions. Our calculations predict, therefore, that there are no ordered $\beta 2(2\times4)$ or $\alpha 2(2\times4)$ phases at finite temperatures in agreement with our experimental results. On the basis of these results we also conclude that the first-order $(2\times4)$-$(4\times2)$ InAs(001) phase transition *cannot* be explained by the attractive As-As interactions proposed by Yamaguchi and Horikoshi.[7,15]

We now turn the discussion to stage II of the transition. Obviously the initial desorption from $\beta 2(2\times4)$ must be followed by further desorption of $As_2$ to convert the surface to a metal-rich stoichiometry. The natural choice for the initial stage of this process is a dimer desorbing directly from $\alpha 2(2\times4)$ (dimer D in Fig. 4). We find the activation energy for this process to be 3.19 eV. However, our theoretical investigation indicates that the activation energy for the desorption of any As dimer generally increases whenever the In atoms supporting that dimer form bonds to additional In atoms, as is the case for the $\alpha 2(2\times4)$ structure. Specifically, removal of the two In atoms in the $\alpha 2(2\times4)$ reduces the activation energy by 370 meV (site E in Fig. 4) to 2.82 eV.

Next, we simulate the full desorption process of an As dimer from the $\beta 2(2\times4)$ reconstructed surface (dimer A in Fig. 4) using DFT. The center-of-mass (c.m.) of the desorbing As dimer is fixed at different points above the surface and all other degrees of freedom are allowed to fully relax, enabling a calculation of the minimum system energy at different heights. The resulting function of the total energy *monotonically increases* with the distance of the c.m. from the surface as seen in Fig. 5. Recent DFT calculations using LDA (Ref. 28) for InAs are in qualitative agreement with our findings. Because no maximum or saddle point is found in the energy, the direct desorption of the As dimer perpendicular to the surface is the optimal, and fastest possible desorption process. This also implies that the calculated adsorption energies for the different dimer positions are identical to the activation energies for desorption.

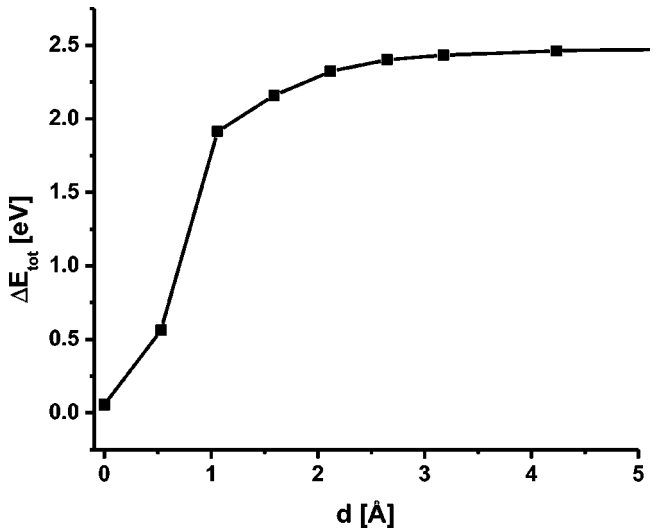


FIG. 5. Total energy of an As dimer desorbing from the $\beta 2(2\times4)$ surface dependent on its center-of-mass distance from the surface.

To show that the As dimer desorption is slower than In atoms leaving the $\alpha 2(2\times4)$ reconstruction, we calculate the energy barrier for removal of an In atom using DFT. We find an upper bound for this process of 1.5 eV, giving a much higher rate than the $As_2$ desorption at the relevant growth temperatures. For higher temperatures, however, we cannot exclude the possibility that the In diffusion will be rate limiting.

## IV. DISCUSSION

In the following we combine the experimental results for static surfaces (STM) with the DFT calculations as input for KMC simulations. The considered microscopic processes for the $(2\times4)$ to $(4\times2)$ phase transition and their interplay are justified by comparing independent experimental (RHEED and STM) and simulated results. The discussion is divided into two stages (Fig. 1) corresponding to the regions of RHEED signature followed by a discussion of the preexponential factor of the As desorption, and comparison to GaAs(001).

### A. Phase transition stage I

To model the surface transition kinetics on the atomic scale we combine individual microscopic processes within a KMC simulation. All KMC parameters that determine the thermodynamical equilibrium are taken from DFT as well as the As-adsorption energies. Based on the results discussed above, the desorption within the KMC model is described by a direct, unimolecular process from surface to vacuum with an activation energy depending only on the local configuration. The DFT results are mapped with no additional free parameters to the As interactions within the KMC simulation including anisotropic nonlinear contributions up to the next nearest in-plane As dimer neighbor. Additionally, As-In interactions influencing the activation energy of the desorption

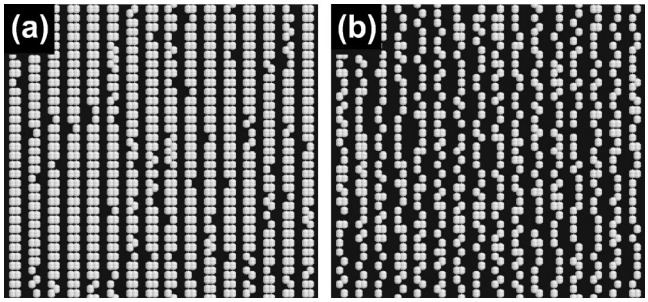


FIG. 6. KMC simulation under identical conditions as used in experiment shown in Fig. 2. Only the top As dimers are shown for clarity.

are included as is the case, e.g., for the dimers D and E in Fig. 4. A full description of the KMC simulation will be published elsewhere.[29]

Only the prefactor for $As_2$ desorption is to be determined by comparison to experiment. We therefore carry out simulations equivalent to the experiments presented in Sec. II. By varying the prefactor within the KMC simulation, the As dimer densities are correlated with those of the STM experiments. In Fig. 2(b) we show an STM image of a surface that is annealed at 420°C for 20 min while exposed to an $As_2$ flux of 0.02 ML/s. From this image, we determine the surface unit cells to be 16% $\beta 2(2\times4)$ and 84% $\alpha 2(2\times4)$, resulting in a top layer As dimer density of 29%. Using the desorption energies determined by DFT, the prefactor required in the KMC simulation to reproduce this dimer density is $\nu = 10^{17}\ s^{-1}$. The simulation result is shown in Fig. 6(b). As a first confirmation that the relevant microscopic processes are included and described with the correct parameters (prefactor, activation energy) we compare the experimental result of Fig. 2(a) to the simulation using identical parameters in Fig. 6(a). The As-dimer density is significantly increased as expected using the higher As flux. The surface is close to the pure $\beta 2(2\times4)$ reconstruction and only a small number of As dimers are missing in quantitative agreement between theory and experiment. If we would have assumed the usual prefactor $\nu = 10^{13}\ s^{-1}$ for the As desorption an activation energy of 1.92 eV for the desorbing $\beta 2(2\times4)$ dimer (dimer D in Fig. 4) would have been necessary to produce the same As dimer density in the simulation at the temperature $T = 420$°C. This value is far outside the error of the DFT calculation ($\pm$ 0.1 eV) that gave 2.48 eV as the activation energy of the same As dimer.

Having determined all parameters for stage I of the surface transition we confirm the suggested As kinetics in a second independent test by comparing to the initial RHEED experiment shown in Fig. 1. Starting from the $\beta 2(2\times4)$ reconstructed surface in the simulation and using the As-desorption prefactor determined above, we monitor the As dimer density during the initial stage of the surface transformation. The close correspondence between specular spot RHEED intensity and simulated As dimer density (see Fig. 7) strongly suggests that the As-desorption process is described correctly. Furthermore, we observe experimentally a reduction of the transition time at higher temperatures although it is difficult to quantify. The faster transition is also

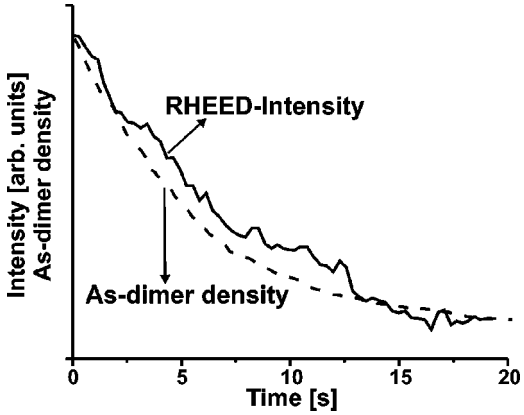


FIG. 7. Comparison of RHEED specular spot intensity (straight line) and As dimer density (dashed) determined from KMC within stage I.

found for our simulation results. We therefore conclude that all theoretical and experimental results are consistent with the desorption of a single As dimer per $(2\times4)$ cell for stage I. In summary, the local reconstruction changes from $\beta 2(2\times4)$ into $\alpha 2(2\times4)$, as shown schematically in Fig. 8.

### B. Phase transition stage II

The experimentally determined activation energy of the $\alpha 2(2\times4)$ to $(4\times2)$ transition $E_A = 2.8\pm0.2$ eV is far lower than the activation energy calculated by DFT for the direct desorption $E_A = 3.19$ eV of dimer D in Fig. 4. However, the activation energy is in good agreement with the desorption process of dimer E. The necessary removal of In atoms from the $\alpha 2(2\times4)$ reconstruction in order to change the local configuration from D to E is found to be much faster for InAs than the As desorption under typical temperatures used in MBE. Therefore, the As desorption is also rate limiting for the transition stage II. The corresponding unusually high prefactor of $\nu = 10^{19}\ s^{-1}$ is also consistent with this As rate limitation. If In diffusion would be rate limiting

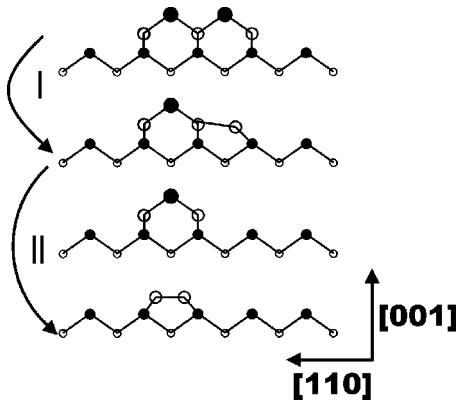


FIG. 8. Schematic of basic processes of the $(2\times4)$ to $(4\times2)$ surface transition. Stage I: Desorption of the $\beta 2(2\times4)$ dimer. Stage II: Removal of In atoms out of the reconstruction followed by desorption of the As dimer.

a prefactor of $\nu = 10^{13}$ s$^{-1}$ would be expected. Figure 8 summarizes the processes involved in stage II of the transition schematically.

### C. Preexponential factor of As desorption

Here we discuss why an unusually high prefactor is not unreasonable for desorption of an As dimer and why the prefactor should be even higher for the second desorbing dimer in stage II. Within transition state theory (TST) the escape rate in a $3N$-dimensional configuration space can be written as[30]

$$\Gamma = k_B T \frac{\int \prod_{i=1}^{3N-1} dq_i dp_i \exp\left(-\frac{H^*}{k_B T}\right)}{\int \prod_{i=1}^{3N} dq_i dp_i \exp\left(-\frac{H}{k_B T}\right)}. \quad (2)$$

The total system is described by its Hamiltonian $H$ around a stable site whereas $H^*$ describes the subsystem excluding the coordinate associated with the transition pathway. This formula allows the calculation of the transition rate knowing the potential energy surface (PES). In principle the full PES could be calculated by DFT. However, this is time consuming due to the large number of degrees of freedom and not attempted here. Instead, we give plausible arguments about what could lead to the unusually high prefactor. Expanding the potential within harmonic approximation around the stable and transition sites leads to the well-known expression by Vineyard[31] [compare to Eq. (1)]

$$\Gamma = \frac{1}{2\pi} \frac{\prod_{i=1}^{3N} \omega_i}{\prod_{i=1}^{3N-1} \omega_i^*} \exp\left(-\frac{E_T - E_B}{k_B T}\right). \quad (3)$$

The fundamental frequencies at the stable site are denoted by $\omega_i$ and at the transition site by $\omega_i^*$. Their ratio determines the total preexponential factor $\nu$. The activation energy $E_A$ is given by the difference between the transition energy $E_T$ and the energy at the stable site $E_B$.

The desorption of an As dimer could be interpreted as a process where the saddle point of the transition is far away from the surface. Hence, the stable site is given by an adsorbed As molecule at the surface whereas the transition state is given by the free As dimer in the vacuum. In vacuum the additional two translational degrees of freedom perpendicular to the desorption pathway only have a weak energetic dependence, implying that their associated fundamental frequencies go to zero. Similar arguments hold for the rotational degrees of freedom (or vibrational degrees at the surface). If the fundamental frequencies of certain modes become small at the transition site with respect to the stable site at the surface then the preexponential factor can only increase. Similar arguments were given also by Sasoka *et al.*[11] These qualitative arguments may explain why we measure an unusually high prefactor; a quantitative investigation, however, needs a complete calculation of the PES.

The different prefactors for the two desorbing As dimers is explainable by the compensation law, or Meyer-Neldel rule (MNR).[32] This law states that within a family of processes following an Arrhenius dependence on temperature, the prefactor $\nu$ obeys the empirical relation

$$\nu = \Gamma_0 \exp\left(\frac{E_A}{E_{MN}}\right), \quad (4)$$

where $\Gamma_0$ is a constant and $E_{\mathrm{MN}}$ is the Meyer-Neldel energy specific to the investigated processes. Therefore, the change of the activation energy is partially compensated by a change of the prefactor. The MNR was shown recently to hold for metal on metal diffusion processes.[33] The higher prefactor for the desorption of the As dimer in stage II of the phase transition indicates that the MNR could also hold for desorption processes from semiconductor surfaces. Moreover, because the transition energy for desorption processes is always identical to the vacuum level, the prefactor might change correspondingly to the adsorption energy of an adsorbate. Qualitatively, the higher activation energy leads to a larger curvature at the adsorption site and therefore to an increase of the prefactor according to Eq. (3).

### D. Comparison to GaAs(001)

Given the similarity between the phase diagrams of InAs(001) and GaAs(001),[4] the question arises why the more typical prefactor of $10^{13}$ s$^{-1}$ is measured for the GaAs $\beta 2(2\times4)$ to $(4\times2)$ transition.[11] Assuming that the microscopic mechanisms are qualitatively similar for both surfaces two principle possibilities exist. Either, the *rate limiting* process for GaAs is also the As desorption or the rate limiting process changes to the removal of the metal atoms. If the rate is limited by As desorption then a qualitatively different behavior of the As dimer on GaAs compared to InAs has to be postulated. This different behavior of the As desorption could be due to the different shape of the PES. Whereas the total energy of the pathway for $As_2$ desorbing from InAs is a monotonic function of the distance to the surface (see above) the PES of $As_2$ desorbing from GaAs was recently found to have an additional maximum.[28]

If Ga atoms limit the total rate, two different explanations can be given why a change of the rate limiting process should occur between InAs and GaAs. First, the relative bond strength between either Ga-Ga or Ga-$As_2$ bonds is different compared to InAs, hence changing the rate limiting process to one controlled by Ga. Second, the ratio of the metal detachment to the $As_2$ desorption rate in stage II of the transition decreases with increasing temperature due to different activation energies and prefactors. Thus, at the higher temperatures typically used for GaAs, Ga detachment could be rate limiting.

## V. SUMMARY

In summary, we have investigated the $(2\times4)$-$(4\times2)$ surface phase transition on InAs(001) and revealed two distinct stages both limited by $As_2$ desorption. Stage I of the transition involves only a unimolecular desorption process of $As_2$ from the $\beta2(2\times4)$ reconstructed surface. Stage II consists of a removal of In and the following desorption of the second $As_2$ molecule. We trace unusually high prefactors deduced from experimental data back to $As_2$ desorption. We find furthermore, that the mixed $\alpha2(2\times4)$-$\beta2(2\times4)$ reconstruction region has no ordered phase at finite temperature.

## ACKNOWLEDGMENTS

We gratefully acknowledge discussions with J.H.G. Owen, C. Ratsch, and R.S. Ross, as well as experimental support by R. Watkins. This work is supported by NSF and DARPA through cooperative agreement DMS-9615854 as part of the Virtual Integrated Prototyping Initiative.

[1] J.E. Northrup and S. Froyen, Phys. Rev. B **50**, 2015 (1994).
[2] A. Kley, Ph.D. thesis, Technische Universität Berlin, (1996).
[3] V.P. LaBella, H. Yang, D.W. Bullock, P.M. Thibado, P. Kratzer, and M. Scheffler, Phys. Rev. Lett. **83**, 2989 (2000).
[4] C. Ratsch, W. Barvosa-Carter, F. Grosse, J.H.G. Owen, and J.J. Zinck, Phys. Rev. B **62**, R7719 (2000).
[5] W.G. Schmidt, S. Mirbt, and F. Bechstedt, Phys. Rev. B **62**, 8087 (2000).
[6] S.-H. Lee, W. Moritz, and M. Scheffler, Phys. Rev. Lett. **85**, 3890 (2000).
[7] H. Yamaguchi and Y. Horikoshi, Phys. Rev. B **51**, 9836 (1995).
[8] J.R. Arthur, Surf. Sci. **43**, 449 (1974).
[9] C.T. Foxon and B.A. Joyce, Surf. Sci. **50**, 434 (1975).
[10] J.Y. Tsao, T.M. Brennan, J.F. Klem, and B.E. Hammons, J. Vac. Sci. Technol. A **7**, 2138 (1988).
[11] C. Sasaoka, Y. Kato, and A. Usui, Appl. Phys. Lett. **62**, 2338 (1993).
[12] B.W. Liang and C.W. Tu, J. Cryst. Growth **128**, 538 (1993).
[13] J.M. Moison, C. Guille, and M. Bensoussan, Phys. Rev. Lett. **58**, 2555 (1987).
[14] T.H. Chiu and J.A. Ditzenberger, Appl. Phys. Lett. **56**, 2219 (1990).
[15] H. Yamaguchi and Y. Horikoshi, Phys. Rev. Lett. **70**, 1299 (1993).
[16] J.H.G. Owen, W. Barvosa-Carter, and J.J. Zinck, Appl. Phys. Lett. **76**, 3070 (2000).
[17] J.H. Neave, B.A. Joyce, and P.J. Dobson, Appl. Phys. A: Solids Surf. **35**, 179 (1984).
[18] J.J. Zinck and D. Chow, Appl. Phys. Lett. **66**, 3524 (1995).
[19] J.J. Zinck, R.S. Ross, J.H.G. Owen, W. Barvosa-Carter, F. Grosse, and C. Ratsch, Appl. Phys. Lett. **79**, 2354 (2001).
[20] W. Barvosa-Carter, R.S. Ross, C. Ratsch, F. Grosse, J.H.G. Owen, and J.J. Zinck, Surf. Sci. **499**, L129 (2002).
[21] G.R. Bell, J.G. Belk, C.F. McConville, and T.S. Jones, Phys. Rev. B **59**, 2947 (1999).
[22] J. Tersoff, M.D. Johnson, and B.G. Orr, Phys. Rev. Lett. **78**, 282 (1997).
[23] M.D. Johnson, K.T. Leung, A. Birch, B.G. Orr, and J. Tersoff, Surf. Sci. **350**, 254 (1996).
[24] D.R. Hamann, Phys. Rev. B **40**, 2980 (1989).
[25] M. Bockstedte, A. Kley, J. Neugebauer, and M. Scheffler, Comput. Phys. Commun. **107**, 187 (1997).
[26] M. Fuchs and M. Scheffler, Comput. Phys. Commun. **116**, 1 (1999).
[27] M. Itoh, G.R. Bell, A.R. Avery, T.S. Jones, B.A. Joyce, and D.D. Vvedensky, Phys. Rev. Lett. **81**, 633 (1998).
[28] R.H. Miwa and G.P. Srivastava, Phys. Rev. B **62**, 15 778 (2000).
[29] F. Grosse and M.F. Gyure, Phys. Rev. B **66**, 075320 (2002).
[30] G. Wahnström, *Rate Equations, Rate Constants and Surface Diffusion*, eidted by V. Borolani, N.H. March, and M.P. Tosi (Plenum Press, New York, 1990), Chap. 16, p. 529.
[31] G.H. Vineyard, J. Phys. Chem. Solids **3**, 121 (1957).
[32] W. Meyer and H. Neldel, Z. Tech. Phys. (Leipzig) **12**, 588 (1937).
[33] G. Boisvert, L.J. Lewis, and A. Yelon, Phys. Rev. Lett. **75**, 469 (1995).